Novel Microbial Fuel Cell Design for raw High Organic Load Waste Water Treatment

Angel Rodrigo Montes Ochoa[1], O. Solarza-Feria[2], J. Tapia-Ramírez[3], K. Sathish-Kumar[1*]

[1]Universidad Politécnica de Aguascalientes, Ingeniería en Energía Calle Paseo San Gerardo No. 207. Fracc. San Gerardo. Aguascalientes, Ags. México, 20342.
[2]Centro de Investigación y de Estudios Avanzados del Instituto Politécnico Nacional, Departamento de Química, Av. Instituto Politécnico Nacional 2508, Col. San Pedro Zacatenco, Delegación Gustavo A. Madero, México D.F. 07360.
[3]Centro de Investigación y de Estudios Avanzados del Instituto Politécnico Nacional, Departamento de Genéticas y Biología Molecular
[*]Tel: +52 4491156589 ; e-mail: sathish.bot@gmail.com,sathishkumarkamaraj@hotmail.com

ABSTRACT

Microbial fuel cells (MFCs) provide new prospects for a sustainable production of energy from organic waste water. Most of the results obtained so far from the field of MFCs research can be exploited to design MFCs. From this context, we proposed the novel simplified softwood based MFC, using pencil was first reported. In pencil, the graphite rod could act as anode besides submerged with wooden portion into the raw high concentrated wastewater solution, and remained wooden portion bound with Pt/Carbon cloth (Cathode) exposed to air. Raw high concentrated waste waters was used both as inoculum to form electrochemically active bacteria on graphite based anode and also as the medium to be treated. Later we treated the softwood with sulphuric acid solution for overnight, tracheids cells lose its cell wall integrity and become swollen in nature. Further, FT-IR spectroscopy confirmed the presence of lignosulfonate on the sulphuric acid treated softwood in the 1032 cm^{-1} and 872 cm^{-1} regions. The conductivity (σ) followed the tendency as 6M sulphuric acid treated softwood < 3M sulphuric acid treated softwood < softwood, and increased almost with the increasing concentration of the sulphuric acid. The volumetric power densities of the novel softwood based MFCs were follows the propensity, 6M sulphuric acid treated softwood (956 mW/m^3) < 3M sulphuric acid treated softwood (212 mW/m^3) < softwood (3 mW/m^3). Thus, the presence of lignosulfonate on the sulphuric acid treated softwood, along with partially hydrolyzed tracheid cell surface bearing SO_3H group mediated proton exchange of both a surface bound proton and a covalently bonded proton between water and hydroxyl, could facilitate the proton exchange. In the case of 3M and 6M sulphuric acid treated softwood MFCs, anodic resistance exhibited higher than the cathode, due to the lower kinetics of the bacterial metabolisms on the anode. However, in softwood MFC showed high cathodic resistance, ascribable to lack of lignosulfonate. From the operation with raw high concentrated wastewater, 6M sulphuric acid treated MFC unveiled superior characteristics of volumetric power density of 1016 mW/m^3 with 19 % columbic efficiency. In addition, eliminating the commercial ion exchange membrane greatly decreases the cost and maintenance for MFC construction, since the costly ion exchange membranes (such as Nafion) contributes a significant portion of capital investment. Thus, this cost-effective feature increases the feasibility for practical application linked with wastewater treatment.

Keywords: microbial fuel cells,proton exchange, aircathode, wastewater treatement.

1. Introduction

Microbial fuel cells are a promising renewable energy production technology, especially in wastewater application, where bacteria act as bio-catalysts to oxidize complex organic or inorganic material to generate electricity, while at the same time the wastewater is treated [1-3]. The increase in MFC power output over the years by several orders of magnitude is a promising trend [4]. However, further increases in power densities are desirable to help improve the economic feasibility of MFC technologies for practical real-world applications [4]. Improved MFCs performance is likely to result from improvements made in optimizing component properties such as anode, cathode, electrolyte and separator (membrane) and reactor configurations. Biocatalysts are capable of directly transferring electrons without the addition of an external mediator to the anode were found in 1999 [5]. Since then, numerous studies of MFCs have been performed, including selection of electrochemically active bacteria, electron-transfer mechanisms, affecting the performance of electric power generation [6].

Many chemicals have been used as electron acceptors in MFCs, but oxygen is the most cost effective, sustainable and environmental friendly electron acceptor for wastewater treatment applications. Cathode design is challenging due to the relatively poor kinetics of oxygen reduction under neutral pH conditions in MFCs, compared to hydrogen fuel cells where cathodes work at much lower pH [7]. Improving cathode performance is therefore critical for increasing power production in MFCs by changes in system architecture that reduce internal resistance, such as by reducing electrode spacing and increasing solution conductivity [8].

Most MFCs require either a closed chamber or two chambers separated by an ion exchange membrane in order to prevent organics or oxidants crossing over to a counter chamber. However, chambered configurations having a membrane show limitations for scaling-up MFCs; for instance, the membrane requires regular cleaning when biofouling or contamination on membrane surface occurs [9]. In addition, closed two chambered MFCs should be designed to ensure that the membrane is not physically damaged by the high hydraulic pressure occurring in large-scale systems; even single-chambered MFCs using air cathodes or membrane electrode assemblies (MEAs) are not free from these challenges. Another concern for fabricating large-scale MFCs and their operation could be the availability of system optimization to minimize the internal resistance of the entire system. The use of one large electrode can cause MFCs to lose cell voltage (i.e., voltage drop) because of the internal resistance and mixed potential formation [10,11].

Among the MFCs components, MFCs reactor configurations is one of the major bottlenecks to high power density and improving its performance is critical to continued development of practical applications. For MFCs to be applied in the energy-recovering wastewater treatment process, both the entire configuration and unit cells should be scalable, moldable, and stackable in series, along with having a low operating cost and be easily serviceable.

We understand this is a first; we employed a softwood material of pencil exploited as integrated membrane via air cathode assembly for real time high concentrated wastewater application. Later we improved the performance of the system treated with sulfuric acid solutions. Moreover, this type of integrated system will have a possibility to scale up the MFCs for conventional wastewater treatment application.

2. Experimental

2.1. Collection of Inoculum

Wastewater was collected from a Universidad Politécnica de Aguascalientes (UPA) and stored in refrigerator at 4°C. The wastewater served as inoculum in anode and also as medium to be treated.

2.2 Construction of novel softwood microbial fuel cell and operation

We took the 5 pencils (4b, 6b, No2), generally protective layer of the graphite made up of softwood material. From that we select the Koh-i-Noor Hardtmuth pencil (Koh-i-Noor Hardtmuth a.s. is a Czech manufacturer and one of the world's largest producers and distributors of a full line of pencils, pens, and art supplies [12]) based on conductivity as well softwood material (Supplementary Table S1.).

Table S1. Electrical measurement of different pencils

No.	Pencils	Image	Resistance (Ω)	Conductivity* (S/m)
1	Conventional Pencil No.2		4.8 Ω	14.88 S/m
2	Pencil - Koh-i-Noor Hardtmuth		2.92 Ω	24.46 S/m
3	Pencil 4b		2.8 Ω	25.51 S/m
4	Pencil 6b		1.64 Ω	43.558 S/m
5	Graphite bar Pencil		1.18 Ω	60.53 S/m

* normalized with the surface area

Far ahead, we peal it off the protective layer (up to 4.2 cm) and remaining graphite could act as anode besides submerged wooden portion (4.2 cm) into the wastewater, remained wooden portion (4.2 cm) bound with Pt/Carbon cloth (0.5mg/cm^2) exposed to air, in order to reduction of oxygen in air to generate water as final by product (Figure 1.). Further, the softwood materials were treated with sulphuric acid solution (3M and 6M) for overnight; then the samples were carefully rinsed with distilled water and left in distilled water for 12 hrs. Earlier, to construct the novel softwood microbial fuel cell using sulphuric acid treated softwood and raw high concentrated wastewater as source of inoculum in all the circumstances. Prominently, we didn´t utilize any external input energy (agitation, circulation, and air purging) in our system (Patent pending).

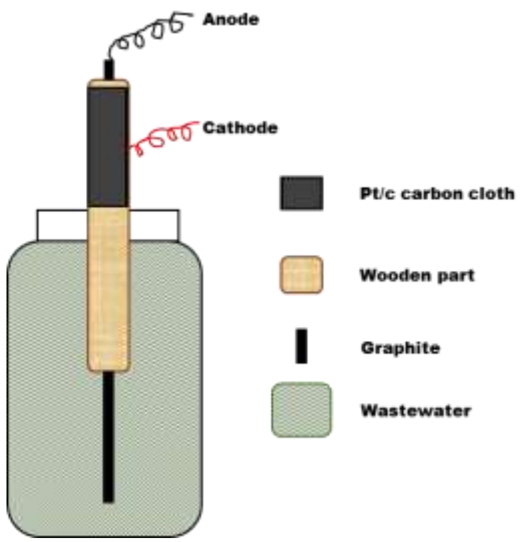

Fig 1. Schematic representation of novel softwood Microbial fuel cell

2.3 Optical microscopy analysis of softwood materials

For optical microscopy, part of the softwood materials was cut in to pieces and immersed in sulphuric acid solution (3M) for overnight. The samples were carefully rinsed with distilled water and left in distilled water for 12 hrs. They were then subjected to dry under ambient conditions. Future, microscopic structures of softwood and sulphuric acid treated softwood were analysed using a MEIJI Techno IM7100.

2.4 Fourier transform infrared (FTIR) spectral analysis of softwood materials

The softwood material and sulphuric acid treated softwood (3M) were characterized with FTIR spectroscopy. FTIR measurements were conducted on an infrared spectrophotometer (Bruker Co., Germany) equipped with an ATR accessory within a range of 4000 to 400 cm^{-1}.

2.5 Conductivity analysis of softwood materials

Proton conductivity of the samples were measured using an AC impedance method with Gamry reference600 Instruments, and the AC frequency ranged from 100 kHz to 10 mHz at a voltage amplitude of 10 mV. A four-electrode system was used to measure the softwood resistance with two outer current carrying electrodes and two inner potential sensing electrodes [13]. With this method the current passed between the two outer electrodes and the resistance was calculated from the AC potential difference between the two inner electrodes. The conductivity was calculated with the following equation:

$$\sigma = \frac{l}{R \times S} \qquad (1)$$

where σ, l, R and S are the proton conductivity, distance between the potential sensing electrodes, resistance of softwood and area and thickness of the membrane in contact with the blocking electrodes respectively. Conductivity measurements were carried out at an ambient temperature with the softwood under fully saturated conditions (100% humidity).

2.6 Electrochemical characterization of novel softwood microbial fuel cells

Novel softwood microbial fuel cell was characterized by linear sweep voltammetry (LSV) and electrochemical impedance spectroscopy (EIS). Liner sweep voltammetry (LSV) was performed in a Gamry Reference 600 Potentiostat/Galvanostat, run at a recommended scan rate of 0.1 mV s^{-1}, starting from the measured open circuit potential up to +50 mV [14,15]. Impedance spectra of microbial fuel cells were obtained at the open circuit potential (E_{ocp}). The amplitude of the signal perturbation was 10 mV, scanned in the frequency range from 100 kHz to 10 mHz. Data fitting was accomplished by Z-view software.

2.7 Analyses

Chemical oxygen demand of the feed and MFC liquor and pH were determined according to the Standard Methods [16]. COD removal efficiency η_{COD} and coulombic efficiency η_{coul} were calculated as reported elsewhere [17]. All the experiments were duplicated.

3. Results and discussion

In generally, pencil cores are made of graphite mixed with a clay binder which leaves grey or black marks, usually protective casing material permanently bonded to the core, which prevents the core from being broken. The protective case material could uses softwood. Softwoods are coniferous trees, such as pines or spruces. Cedar wood (*Calocedrus decurrens* (*syn. Libocedrus decurrens*)) is most commonly used in pencil production [18].

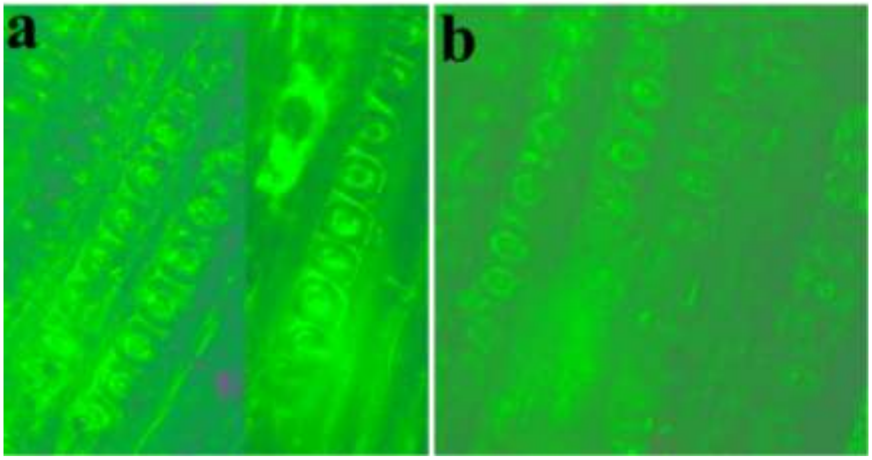

Fig 2. Optical microscopy images of softwood. a) Softwood b) Softwood treated with sulphuric acid

Softwood cellular structure is simple and 90-95 percent of the cells are longitudinal tracheids, longitudinal tracheids function in water conduction and support. The limited number of cell types makes softwoods more difficult to differentiate from one another [19]. Figure 2 shows the optical images of the longitudinal structure of the tracheids. Softwood exhibited the well-defined cell walls structure of the longitudinal tracheids cell (Fig 2.(a)), after the overnight treatment with sulphuric acid (3M) loses its cell wall integrity and become swollen (Fig 2.(b)).

The FT-IR spectra for the softwood and sulphuric acid tread softwood were explicit in Figure 3. The FTIR spectra of softwood (Fig 3.) showed a broadening to lower wavenumbers of the band at 3320 cm^{-1} corresponding to the O-H stretching vibration from alcohols (3600-3300 cm^{-1}) and carboxylic acid (3300-2500 cm^{-1}), present either in polysaccharides and lignin. In treated softwood exhibited slightly broader band at 3335 cm^{-1} and slightly increased sharpen band at 2925 cm^{-1} -2850 cm^{-1}. This could be speculated to the slight increase in carboxylic acids due to primary OH oxidation and/or hydrolysis of acetyl groups from hemicelluloses. Moreover the change of O-H stretching frequencies can also be due to the modification of cellulose crystallinity influenced by dehydration effects [20 ,21]. Even though O-H stretch due to polysaccharides could decrease, at the same time O-H from phenolic groups in lignin increases since it is a well fact that the lignin percentage increases due to carbohydrate degradation [22].

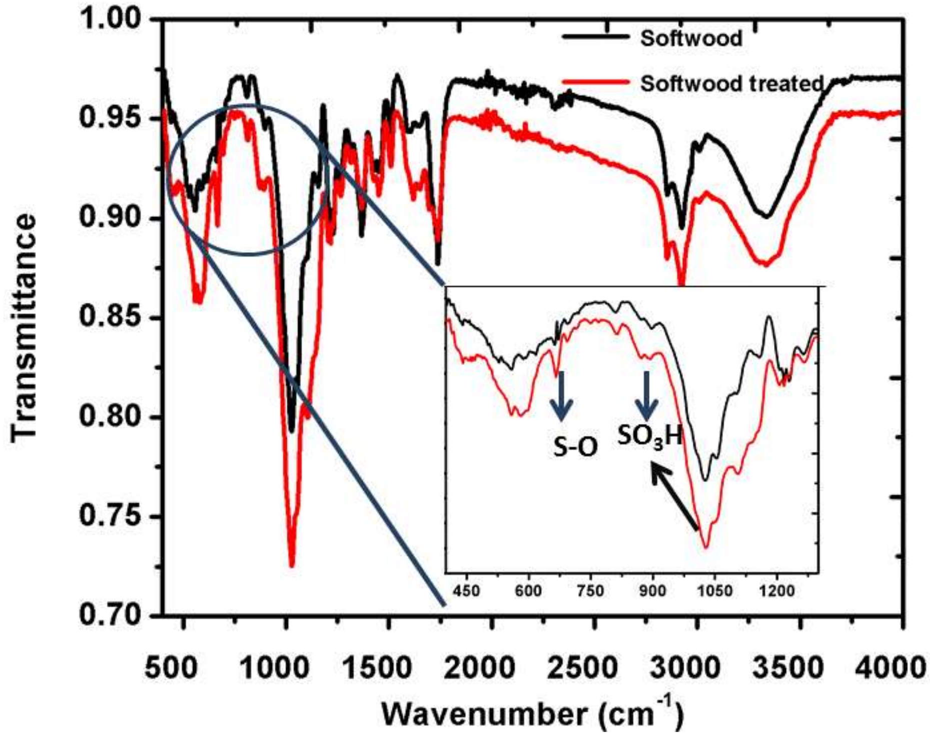

Fig 3. FTIR Spectrum of the softwood and sulphuric acid treated softwood, Inset- Footprint region of sulfonyl group

The two bands at 2900-2800 cm^{-1} are composed by the overlapping of the stretch asymmetric vibration of $–CH_2$ (2935-2915 cm^{-1}) and $–CH_3$ (2970-2950 cm^{-1}) and by the overlapping of stretch symmetric vibrations of $–CH_2$ (2865-2845 cm^{-1}) and $–CH_3$ (2880-2860 cm^{-1}). Untreated softwood showed the stretch asymmetric vibration of $–CH_2$ at 2925 cm^{-1} and $–CH_3$ at 2970 cm^{-1} and symmetric stretch at 2855 cm^{-1} of $–CH_2$. Normally the asymmetric band shows a higher absorptivity. The treated softwood shows evident disappear of frequency at 2970 cm^{-1} of $–CH_3$ and, slightly increase frequency at 2925 cm^{-1} of $–CH_3$ and 2852 cm^{-1} of $–CH_2$ bands are due to structural and relative composition changes, particularly at cellulose crystallinity level with influence of C-H and O-H stretch frequencies [20,21] and changes in the relative importance of lignin methoxyl groups for which the CH_3 stretching vibrations have lower CH stretching frequencies [23].

According to Mitchell and Higgins (2002) [24], the band around 1730 cm^{-1} is almost exclusively due to carbonyl group of acetoxy groups in xylan. In the spectra of untreated softwood shows sharp peak at 1735 cm^{-1} and treated softwood shows band decreases might be due to the breaking of hemicelluloses specifically acetyl or acetoxy groups in xylan. Similar results were obtained by Tjeersdsma and Militz (2005) [25].

The band at 1595 cm^{-1} corresponds to vibrations in the aromatic ring of lignin plus C=O stretching. The band at 1595 cm^{-1} broadens to about 1615 cm^{-1} for treated softwood but not for untreated softwood. This peak shifting suggests that there was an increase of structural diversity around the aromatic rings, absorbing at a greater range of frequencies. The height of the band slightly increase only in the spectrum of treated softwood, might be an increase in the percentage of lignin in treated wood [26,27].

Aromatic rings exhibited band at 1510 cm^{-1} for softwood lignin (Guaiacyl- G) [28]. Fig 3. Shows the treated softwood exhibited the slightly increase peak at 1510 cm^{-1}, Also confirmed the increase the content of lignin after the acid treatment.

The band at 1460 cm^{-1} corresponds to the asymmetric deformation of C-H bond of xylan, while the band at 1420 cm^{-1} corresponds to the vibration of the aromatic ring of lignin [24]. Untreated softwood shows the peak at 1460 cm^{-1} corresponds to xylan. Interestingly, treated softwood exhibited two bands at 1460 $cm^{-1}$of $–CH_3$ and 1420 cm^{-1} of lignin. This could be speculated the effect of sulphuric acid on hemicellulose decrease and lignin peak arises.

The band at 1330 cm^{-1} represents the contributions of all structural components of wood because it corresponds to C-H bending of polysaccharides which joins the bands at 1327 cm^{-1} of S lignin condensed units [28]. There was a clear intense peak observed in treated softwood at 1330 cm^{-1} corresponding to an increase in lignin condensation. The report was corroborated by Windeisen et al., 2007 [29].

For treated softwood the band at 1240 cm^{-1} decreased in height, which once again confirms the existence of a more condensed structure [29,30]. This band has a shoulder at 1145 cm^{-1} with G lignin and 1105 cm^{-1} with GS lignin [28].

The peak at 897 cm^{-1} corresponding to the sugar ring tension, seemed to decrease with treated softwood treatment which is consistent with ring opening. Similar results were obtained by Kotilainen et al., 2000 [26], Gonzalez-Peña et al., 2009 [31]. The band appearing at 620-660 cm^{-1} is assigned to the sulfonic groups (S-O stretching vibration) formed from the reaction of sulphuric acid with the secondary OH of the aliphatic side chain of lignin's [32], formed on sulphuric acid treated softwood. The FT-IR spectrum of the SO_3H group-bearing sulphuric acid treated softwood is shown in the Figure 3. The peaks due to the SO_3H group are seen at 1032 cm^{-1} and at 872 cm^{-1}. Thus, confirmed the presence of lignosulfonate on the sulphuric acid treated softwood [33].

Figure 4. Illustrate the proton conductivity of the softwood, 3M sulphuric acid treated softwood and 6M sulphuric acid treated softwood. From the proton conductivity (σ) study, the value of the σ followed the tendency as 6M sulphuric acid treated softwood < 3M sulphuric acid treated softwood < softwood and increased almost with the increasing concentration of the sulphuric acid. It is well-known that SO_3H group bearing materials like Amberlyst-15 can be used as a cation exchanger [34-36]; therefore the sulfonated softwood materials also exhibited the high proton conductivity in 6M sulphuric acid treated softwood (10.8 mS/cm^2).

The polarization curve of the softwood, 3M sulphuric acid treated softwood and 6M sulphuric acid treated softwood based novel softwood MFCs were shown in figure 5. The volumetric power densities was follows the propensity, 6M sulphuric acid treated softwood (956 mW/m^3) < 3M sulphuric acid treated softwood (212 mW/m^3) < softwood (3 mW/m^3) (Table 1. Fig 5.). This behaviour could follow the conductivity results. Thus, the presence of lignosulfonate on the sulphuric acid treated softwood (Fig 3), along with partially hydrolysed tracheid cell surface bearing SO_3H group mediated proton exchange of both a surface bound proton and a covalently bonded proton between water and hydroxyl, could facilitate the proton exchange [37]. Further, the integrated membrane cathode enables a unidirectional flow, which improves proton transfer through convection. In addition, eliminating the commercial ion exchange membrane greatly decreases the cost and maintenance for MFC construction, since the costly ion exchange membranes (such as Nafion) contributes a significant portion of capital investment. Thus, this cost-effective feature increases the feasibility for practical application linked with wastewater treatment.

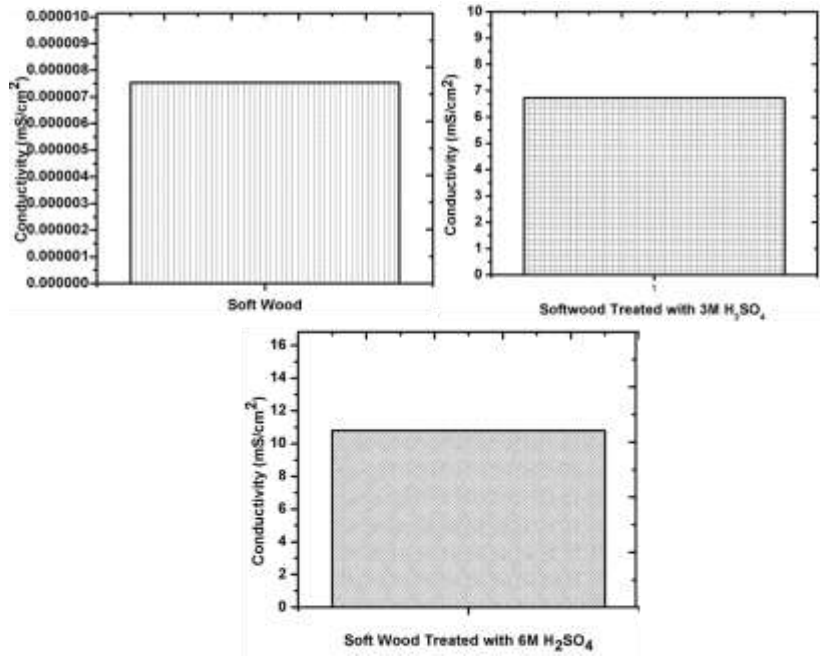

Fig 4. Conductivity of Softwood, Softwood treated with 3M and 6M of H_2SO_4

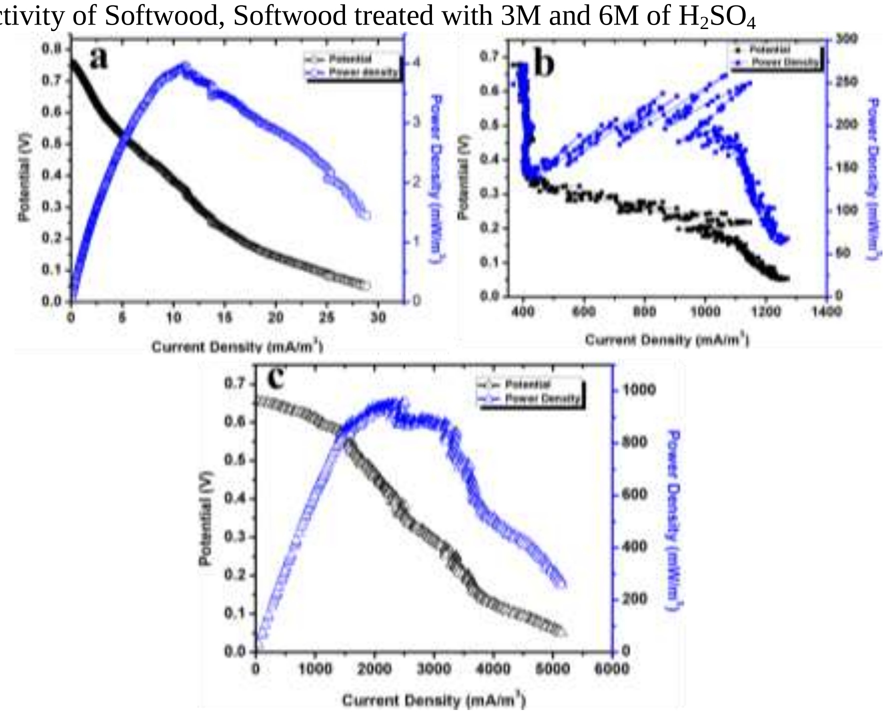

Fig 5. Polarization curve of Softwood (a), 3M treated H_2SO_4 (b) and 6M treated H_2SO_4 (c)

Table 1. Electrochemical characterization of novel softwood Microbial fuel cells

Types	I_{max} (mA)	P_{max} (mW)	$P_{v\text{-}max}$ [a] (mW/m^3)	$I_{s,max}$ [b] (mA/m^3)	E_{max} (V)	R_{anode} (Ω)	$R_{cathode}$ (Ω)	$R_{softwood}$ (Ω)	R_{int}(Ω)
Softwood	0.00099 ±4	0.00033 ±7	3±81	9±43	0.403 ±2	358±3	15175 ±42	26504±65	42037±52
3M H_2SO_4 treated Softwood	0.095 ±3	0.023 ±6	212± 63	863± 47	0.246 ±5	138±1	46±03	582±2	766±2
6M H_2SO_4 treated Softwood	0.276 ±2	0.105 ±2	956± 22	2511± 22	0.381 ±3	364±8	5±6	260±4	629±6

Note: [a] maximum volumetric power density; [b] maximum volumetric current density.

Electrochemical impedance spectroscopy of the novel softwood based MFCs are shown in Figure 6.the inset explicit the equivalent circuit fitted by Z-view. In the case of 3M and 6M sulphuric acid treated softwood MFCs, anodic resistance exhibited higher than the cathode, due to the lower kinetics of the bacterial metabolisms [38] on the anode. However, in softwood MFC showed high cathodic resistance, ascribable to lack of lignosulfonate (Table 1.).

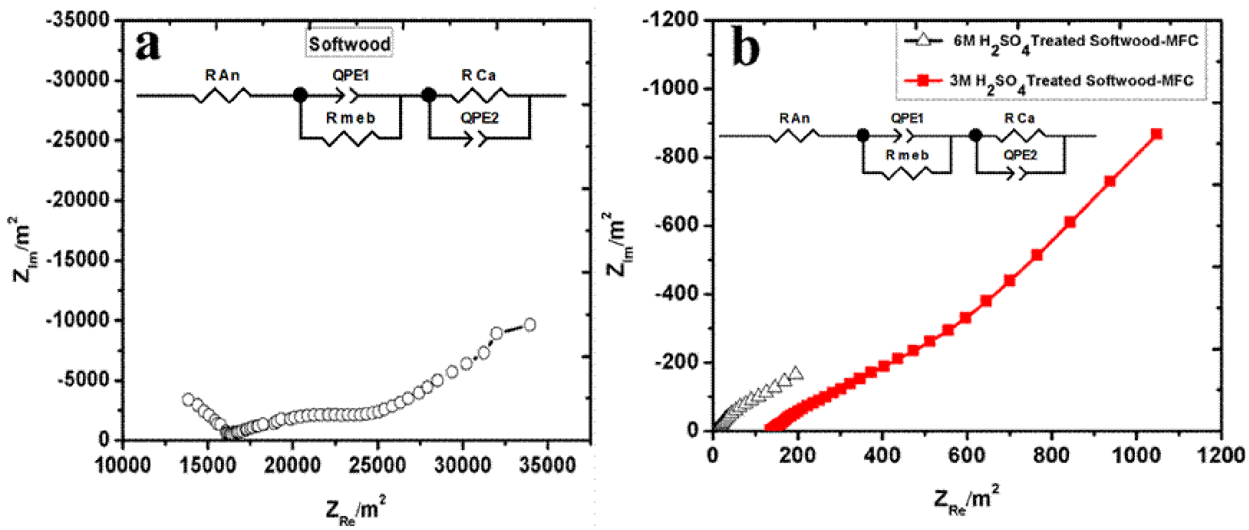

Fig 6. Electrochemical Impedance Spectroscopy of Softwood (a) and 3M H_2SO_4 [□], 6M H_2SO_4 [Δ] (b). Inset: Equivalent Circuit

Later, we operate the novel softwood based MFCs with high concentrated raw wastewater solution as sole carbon source and biocatalyst. Figure 7. Demonstrated the closed circuit operation of the novel

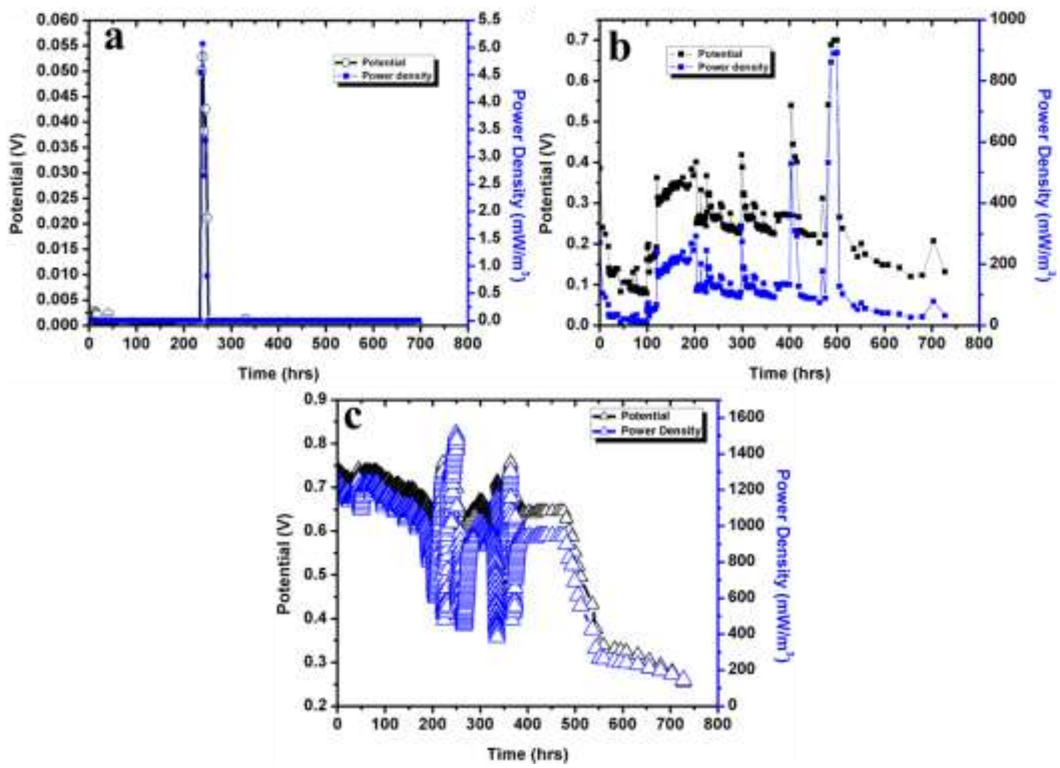

Fig 7. Closed circuit operation of Softwood (a), 3M H_2SO_4 (b) and 6M H_2SO_4 (c)

Table 2. Average values of parameters in operation of the novel softwood microbial fuel cell. Standard deviations were calculated with respect to time of operation.

Parameters	Softwood	3M H_2SO_4 treated Softwood	6M H_2SO_4 treated Softwood
P^a (mW/m^2)	0.0101±0.1	22.19±22	249.49±5
$P_V{}^b$ (mW/m^3)	0.0514±0.45	118.63±11	1016.11±202
P^c (mW)	0.0000056±4	0.0130±2	0.112±2
I (mA/m^2)	0.313±1	83.82±36	370.99±39
I (mA/m^3)	1.592±3	425.81±19	1510.95±162
I^d (mA)	0.000175±1	0.0468±1	0.166±2
E^e (V)	0.000876±0.005	0.234±0.1	0.665±0.8
$\eta_{COD}{}^f$ (%)	80.6	84.6	92.3
$\eta_{Coul}{}^g$ (%)	3	16	19

Notes: [a] surface area power density; [b] volumetric power density; [c] average power; [d] average current; [e] average potential; [f] chemical oxygen demand removal efficiency; [g] coulombic efficiency.

softwood based MFCs for 700 hrs. Their average parameters values were in Table 2. 6M sulphuric acid treated MFC unveiled superior characteristics such as volumetric power density of 1016 mW/m^3 with 19 % columbic efficiency, among the other softwood based MFCs. Despite of the low columbic efficiency, especially during the treatment of real wastewater, had one of the following reasons: 1.entrapment and accumulation of organic particles from wastewater in the anodic biofilm [39]; 2. Production of methane [40]; 3. Losses in efficiency due to the energetic requirements to sustain fermentative and acetogenic communities in the anodic food web [41]; and 4. Diffusion of the terminal electron acceptor oxygen into the anode [42].

4. Summary and perspectives

The simplified novel softwood based microbial fuel cell using pencil was first reported. In pencil, the graphite rod could act as anode besides submerged with wooden portion into the raw high concentrated wastewater solution, and remained wooden portion bound with Pt/Carbon cloth (Cathode) exposed to air. Raw high concentrated waste waters was used both as inoculum to form electrochemically active bacteria on graphite based anode and also as the medium to be treated. Later we treated the softwood with sulphuric acid solution for overnight, lose its cell wall integrity and become swollen in nature. Further, FT-IR spectroscopy confirmed the presence of lignosulfonate on the sulphuric acid treated softwood in the 1032 cm^{-1} and 872 cm^{-1} regions. The proton conductivity (σ) followed the tendency as 6M sulphuric acid treated softwood < 3M sulphuric acid treated softwood < softwood, and increased almost with the increasing concentration of the sulphuric acid. The volumetric power densities of the novel softwood based MFCs were follows the propensity, 6M sulphuric acid treated softwood (956 mW/m^3) < 3M sulphuric acid treated softwood (212 mW/m^3) < softwood (3 mW/m^3). Thus, the presence of lignosulfonate on the sulphuric acid treated softwood, along with partially hydrolysed tracheid cell surface bearing SO_3H group mediated proton exchange of both a surface bound proton and a covalently bonded proton between water and hydroxyl, could facilitate the proton exchange. In the case of 3M and 6M sulphuric acid treated softwood MFCs, anodic resistance exhibited higher than the cathode, due to the lower kinetics of the bacterial metabolisms on the anode. However, in softwood MFC showed high cathodic resistance, ascribable to lack of lignosulfonate. From the operation with raw high concentrated wastewater for 700 hrs, 6M sulphuric acid treated MFC unveiled superior characteristics such as volumetric power density of 1016 mW/m^3 with 19 % columbic efficiency. In addition, eliminating the commercial ion exchange membrane greatly decreases the cost and maintenance for MFC construction, since the costly ion exchange membranes (such as Nafion) contributes a significant portion of capital investment. Thus, this cost-effective feature increases the feasibility for practical application linked with wastewater treatment.

Acknowledgements

The author KSK would like to acknowledge the Universidad Politécnica de Aguascalientes (UPA) and CINVESTAV-IPN, Zacatenco, D.F, for provided the necessary equipment for the characterisation. We thank the Programa de Apoyo al Desarrollo de la Educación Superior (PADES) of SECRETARíA DE EDUCACiÓN PÚBLICA (SEP), Mexico for funding this research work (Número de proyecto: 2014-01-01-002-039-Apoyo para adquisición de equipo e ins1rumentación para el desarrollo de celdas de combustible microbianas). We thank Dr. José Gerardo Cabañas Moreno for his technical assistance with operation of FT-IR Spectroscopy. We are grateful to the excellent technical assistance from, Ing. Andrés Rodríguez-Castellanos, Ing. Sebastián Citalán Cigarroa, and Mr.Julio cesar magallon, Dept. of Chemistry, Mr. Victor Tapia, Dept. of Genetics and Molecular Biology, CINVESTAV-IPN, Zacatenco. Mexico,D.F. and Ing. Alejandro De la Torre, (data collection using Arduino) UPA. We also acknowledge the Dr. Andres Antonio Torres Acosta and SATELsa S.A de C.V (RENIECYT) for lending the Gamry Instruments Reference 600.

References

[1] A. L. Vazquez-Larios, O. Solorza-Feria, G. Vazquez-Huerta, F. Esparza-Garcia, E. Rios-Leal, N. Rinderknecht-Seijas, H. M. Poggi-Varaldo, A new design improves performance of a single chamber microbial fuel cell. J. New mater. Electrochem. Syste 2010; 13(3): 219-226.
[2]R. Navanietha Krishnaraj, S. Berchmans, P. Pal, Symbiosis of photosynthetic microorganisms with non-photosynthetic ones for the conversion of cellulosic mass into electrical energy and pigments. Cellulose 2014; 21:2349-2355.
[3] K. Sathish-Kumar, O. Solorza-Feria, J. Tapia-Ramı´rezc, N. Rinderkenecht-Seijas, H. M. Poggi-Varaldo, Electrochemical and chemical enrichment methods of a sodicesaline inoculum for microbial fuel cells. Inter. J. Hydrogen Energy 2013; 38:12600-12609.
[4]A. Rinaldi, B. Mecheri, V. Garavaglia, S. Licoccia, P. Di Nardo, E. Traversa, Engineering materials and biology to boost performance of microbial fuel cells: a critical review. Ener. Environ Sci 2008; 1:417-429.
[5] B.H. Kim, H.J. Kim, M.S. Hyun, D.H. Park, Challenges in microbial fuel cell development and operation. J. Microbiol. Biotechnol. 9 (1999) 127–131.
[6]K. Sathish-Kumar, O. Solorza-Feria, G. Vázquez-Huerta, J.P. Luna-Arias, and H.M. Poggi-Varaldo. Electrical Stress-Directed Evolution of Biocatalysts Community Sampled from a Sodic-Saline Soil for Microbial Fuel Cells. J. New Mater. Electrochem Syst. 2012;15: 181-86.
[7]J. Reyes-Rodríguez, F. Godínez-Salomón, M. Leyva, Solorza-Feria O. RRDE study on Co@ Pt/C core–shell nanocatalysts for the oxygen reduction reaction. International Journal of Hydrogen Energy 2013; 38:12634-12639.
[8]Z. Hu. Electricity generation by a baffle-chamber membraneless microbial fuel cell. Journal of Power Sources 2008;179:27-33.
[9]J. Xu, G.-P. Sheng, H.-W. Luo, W.-W Li, L.-F Wang, H.-Q. Fouling of proton exchange membrane (PEM) deteriorates the performance of microbial fuel cell. Water Research 2012;46:1817-1824.
[10]A. Dewan, H. Beyenal and Z. Lewandowski. Scaling up microbial fuel cells. Environ. Sci. Technol 2008;42(20): 7643-8.
[11]F. Harnisch, S. Wirth, U. Schroder. Effects of substrate and metabolite crossover on the cathodic oxygen reduction reaction in microbial fuel cells: platinum vs. iron(II) phthalocyanine based electrodes. Electrochem. Commun 2009;11: 2253–2256.
[12] http://www.koh-i-noor.cz/en/
[13]S. Slade, S.A. Campbell, T.R. Ralph, F.C. Walsh. Ionic Conductivity of an Extruded Nafion 1100 EW Series of Membranes. Journal of The Electrochemical Society 2002;149:A1556-A1564.
[14] S.B. Velasquez-Orta, T.P. Curtis, B.E. Logan. Energy from algae using microbial fuel cells. Biotechnol Bioeng 2009;103(6): 1068-76.
[15]V.J. Watson, B.E. Logan. Analysis of polarization methods for elimination of power overshoot in microbial fuel cells. Electrochem Commun 2011;13(1): 54-6.
[16]APHA. Standard methods for examination of water and wastewater. 17th ed. Washington DC: American Public Health Association; 1981.
[17]J.J. Fornero, M. Rosenbaum, L.T. Angenent. Electric Power Generation from Municipal, Food, and Animal Wastewaters Using Microbial Fuel Cells. Electroanalysis 2010;22:832-843.
[18] http://education.nationalgeographic.com/education/?ar_a=1
[19]R.B. Hoadley. Identifying Wood: Accurate Results with Simple Tools. Taunton Press, Inc. Newton, CT. 1990.
[20]M. Moharram, O. Mahmoud. FTIR Spectroscopic Study of the Effect of Microwave Heating on the Transformation of Cellulose I into Cellulose II during Mercerization. Journal of Applied Polymer Science 2008;107(1): 30-36.
[21]I. Spiridon, C. Teacă, R. Bodîrlău. Structural changes evidenced by FTIR spectroscopy in cellulosic materials after pre-treatment with ionic liquid and enzymatic hydrolysis. Bioresources 2011;6(1):400-413.
[22]B. Esteves, R. Videira, H. Pereira. Chemistry and ecotoxicity of heat treated pine wood extractives, Wood Sci Technol 2011;45 (6):661-676.
[23]J. Coates. Interpretation of Infrared Spectra, A Practical Approach in Encyclopedia of Analytical Chemistry. R.A. Meyers (Ed.). John Wiley & Sons Ltd. pp. 2000;10815-10837
[24]A. Michell, H. Higgins. Infrared Spectroscopy in Australian Forest Products research. CSIRO Forestry and Forest Products, Melbourne, Australia 60p. 2002.
[25]B. Tjeerdsma, H. Militz. Chemical changes in hydrothermal treated wood: FTIR analysis of combined hydrothermal and dry heat-treated wood. Holz als Roh- und Werkst 2005;63(2): 102-111.
[26]R. Kotilainen, T. Toivannen, R. Alén. FTIR monitoring of chemical changes in softwood during heating. Journal of Wood Chemistry and Technology 2000;20(3): 307-320.
[27]J. Li, B. Li, X. Zhang. Comparative studies of heat degradation between larch lignin and Manchurian ash lignin. Polymer Degradation and Stability 2002;78: 279-285.

[28]O. Faix. Classification of lignins from different botanical origins by FT-IR spectroscopy. Holzforschung 1991;45 (1): 21-27.
[29]E. Windeisen, C. Strobel, G. Wegener. Chemical changes during the production of thermotreated beech wood. Wood Sci Technol 2007;41(6): 523-536.
[30]D. Kocaefe, S. Poncsak, Y. Boluk. Effect of thermal treatment on the chemical compositionand mechanical properties of birch and aspen. Bioresources 2008;3(2): 517-537.
[31]M.M. González-Peña, S.F. Curling, M.D.C. Hale. On the effect of heat on the chemical composition and dimensions of thermally-modified wood. Polymer Degradation and Stability 2009;94(12): 2184-2193.
[32]P. Rodríguez-Lucena, J.J. Lucena, L. Hernández-Apaolaza. Relationship between the structure of Fe-Lignosulfonate complexes determined by FTIR spectroscopy and their reduction by the leaf Fe reductase. The Proceedings of the International Plant Nutrition Colloquium XVI. UC Davis: Department of Plant Sciences, UC Davis. 2009.
[33]D. Lee. Preparation of a Sulfonated Carbonaceous Material from Lignosulfonate and Its Usefulness as an Esterification Catalyst. Molecules 2013;18:8168-8180.
[34]C.B. Campbell, A. Onopchenko. Cation-exchange resin (Amberlyst-15) catalyzed alkylation of phenol with unhydrogenated PAO decene trimer. Rearrangement of tert-alkylphenols to sec-alkylphenols. Industrial & Engineering Chemistry Research 1992;31:2278-2281.
[35]X. Zang, Z. Zhang, F. Wang, Y. Wang, Q. Song, J. Xu. Lignosulfonate-based heterogeneous sulfonic acid catalyst for hydrolyzing glycosidic bonds of polysaccharides. J. Mol. Catal. A-Chem. 2013;377:102–107.
[36]F. Liu, J. Sun, Q. Sun, L. Zhu, L. Wang, X. Meng, C. Qi, F.S. Xiao. High-temperature synthesis of magnetically active and SO H-functionalized ordered mesoporous carbon with good catalytic performance. Catal. Today 2012;186:115–120.
[37]X.L. Hu, J. Klimes, A. Michaelides. Proton transfer in adsorbed water dimers. Physical Chemistry Chemical Physics 2010;12:3953-3956.
[38]K. Sathish-Kumar, O. Solorza-Feria, R. Hernández-Vera, G. Vazquez-Huerta, and H.M. Poggi-Varaldo, Comparison of Various Techniques to Characterize a Single Chamber Microbial Fuel Cell Loaded with Sulfate Reducing Biocatalysts Journal of New Materials for Electrochemical Systems 2012b; 15: 195-201.
[39]K. Rabaey, P. Clauwaert, P. Aelterman, W. Verstraete. (2005). Tubular microbial fuel cells for efficient electricity generation. Environ. Sci. Technol 2005; 39(20): 8077.
[40]Z. He, S.D. Minteer, L.T. Angenent. Electricity generation from artificial wastewater using an upflow microbial fuel cell.
Environ. Sci. Technol 2005; 39: 5262-5267.
[41]B. Min, B.E. Logan. Continuous Electricity Generation from Domestic Wastewater and Organic Substrates in a Flat Plate Microbial Fuel Cell. Environmental science & technology 2004;38:5809-5814.
[42]B. Min, J. Kim, S. Oh, J.M. Regan, B.E. Logan. Electricity generation from swine wastewater using microbial fuel cells. Water Research 2005;39:4961-4968.